Article

Probing for and Quantifying Agonist Hydrogen Bonds in #6#2 Nicotinic Acetylcholine Receptors

Michael Post, Henry A Lester, and Dennis A. Dougherty

Biochemistry, **Just Accepted Manuscript** • Publication Date (Web): 13 Mar 2017

Probing for and Quantifying Agonist Hydrogen Bonds in α6β2 Nicotinic Acetylcholine Receptors

Post, Michael R.*, Henry A. Lester‡, Dennis A. Dougherty*

**Division of Chemistry and Chemical Engineering; ‡Division of Biology and Biological Engineering, California Institute of Technology, Pasadena, CA 91125 USA*

Abstract

Designing subtype-selective agonists for neuronal nicotinic acetylcholine receptors (nAChR) is a challenging and significant goal aided by intricate knowledge of each subtype's binding patterns. We previously reported that in α6β2 receptors, acetylcholine makes a functional cation-π interaction with Trp149, but nicotine and TC299423 do not, suggesting a distinctive binding site. This work explores hydrogen binding at the backbone carbonyl associated with α6β2 Trp149. Substituting the *i+1* residue, Thr150, with its α-hydroxy analogue (Tah) attenuates the carbonyl's hydrogen bond accepting ability. At α6(T150Tah)β2, nicotine shows a 24-fold loss of function, TC299423 shows a modest loss, and acetylcholine shows no effect. Nicotine was further analyzed via a double-mutant cycle analysis utilizing N'-methylnicotinium, which indicated a hydrogen bond in α6β2 with a ΔΔG of 2.6 kcal/mol. Thus, even though nicotine does not make the conserved cation-π interaction with Trp149, it still makes a functional hydrogen bond to its associated backbone carbonyl.

Graphical Abstract:

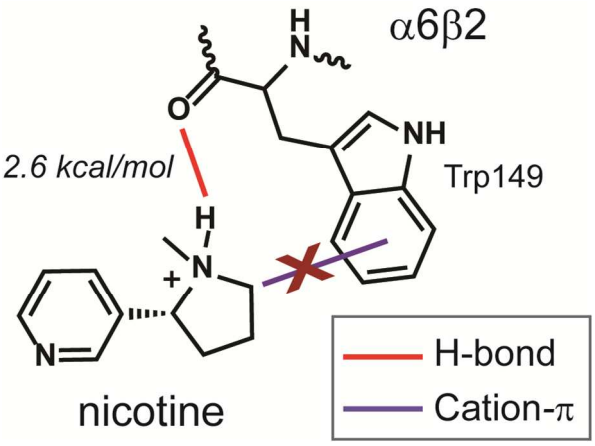

Introduction

The neuronal nicotinic acetylcholine receptors (nAChRs) are a group of pentameric ligand-gated ion channels (pLGICs) typically found at presynaptic terminals, where they modulate neurotransmitter release.[1–3] There are eleven known subunits – α2 through α7, α9, α10 and β2 through β4 – that assemble into pentamers in different combinations.[4] The different subunits share a common topology, and the agonist binding site is found in the extracellular binding region at the interface of two subunits. Different subunit combinations, i.e. different nAChR subtypes, display distinctive functions, pharmacologies, and localizations.[5] While several subtypes are distributed throughout the brain (e.g. α4β2 and α7), others are concentrated in specific regions and only expressed by certain cell types.[6,7] The α6-containing subtypes follow the latter pattern and are prominently expressed in dopaminergic neurons of the ventral tegmental area and the substantia nigra pars compacta, making them promising targets for both Parkinson's disease and addiction.[8–10] In addition, the α6 subunit is expressed in dorsal root ganglia, where it plays an important role in mechanical allodynia associated with neuropathies and inflammatory injuries.[11] As such, insights into strategies for targeting drugs specifically to α6-containing nAChRs would be quite valuable.

Mapping the binding interface is a major step toward that goal. An increasing collection of structural data has provided valuable guidance, but it has been less helpful in revealing the subtle features that distinguish particular subtypes. For prototype agonists such as ACh and nicotine (structures shown in Figure 1A), the residues comprising the primary and complementary binding interfaces are conserved among all α and all β subunits, respectively.[12] Therefore, additional precision is required to understand the functional details of neuronal nAChR binding sites.[13] We have established a strategy based on the incorporation of non-

canonical amino acids and electrophysiological characterization that allows high precision characterization of drug-receptor interactions in nAChRs and related systems.[14] Application of this approach to the α4β2 nAChR – the most common nicotinic receptor in the brain – revealed three key binding interactions: a cation-π interaction with α4 Trp149, a hydrogen bond with the backbone carbonyl associated with Trp149, and an additional hydrogen bond between nicotine's pyridine nitrogen and a backbone NH in the β2 subunit.[15,16] The cation-π interaction at Trp149 – which is also referred to as TrpB as it lies on the canonical "loop B" of the primary agonist binding site – has been observed at homologous aromatic residues throughout the nAChR and broader pLGIC families and was later corroborated in recent crystal structures of α4β2 nAChR, glycine, and serotonin receptors.[17–21] Yet, recent work using non-canonical amino acid mutagenesis has shown that in the α6β2 receptor, acetylcholine makes a functionally important cation-π interaction, but nicotine and TC299423 (an agonist that shows some selectivity for α6β2 receptors,[22] structure shown in Figure 1A) do not.[23] This binding mode differs from the α4β2 subtype, which suggests the question: what other interactions besides a cation-π interaction at Trp149 might be responsible for the binding of nicotine and TC299423 in the α6β2 nAChR?

This report investigates the role of a possible hydrogen bond between an agonist's amine moiety and the backbone carbonyl associated with TrpB in α6β2. While quaternary ammonium agonists such as acetylcholine are unable to make a hydrogen bond, such interactions have been observed in α4β2 for nicotine and the smoking cessation drugs varenicline (Chantix®) and cytisine (Tabex®),[24,25] all of which contain a protonated amine (ammonium ion) that provides the hydrogen bond donor. In each of those instances, evidence of the hydrogen bond was accompanied by evidence of a cation-π interaction at TrpB; however, because nicotine was not observed to make a strong cation-π interaction at TrpB with α6β2, it was uncertain whether it

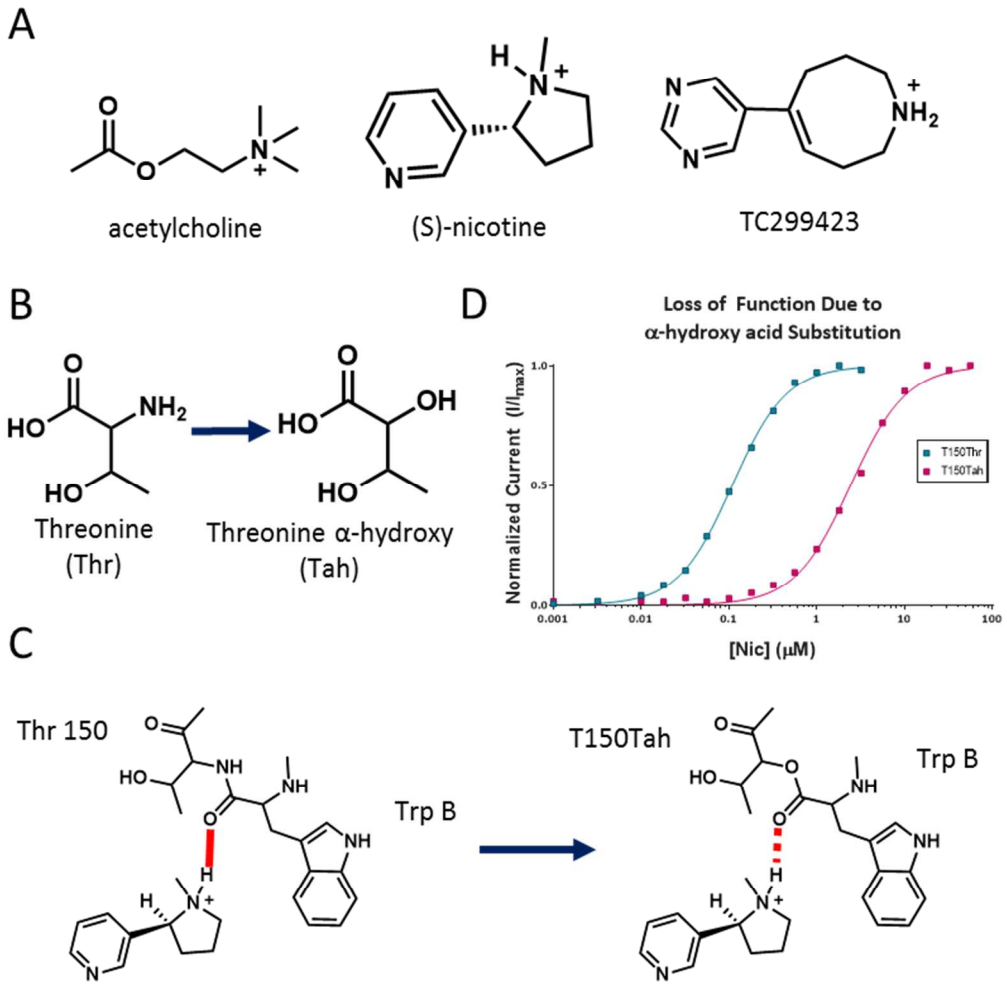

Figure 1. A) Agonists used to probe for hydrogen bonds with Trp149-associated backbone carbonyl in α6β2. B,C) Probing H-bonds uses the Tah strategy, which effectively mutates the amide backbone into an ester bond. D) A functional hydrogen bond results in an increase in EC_{50} in the Tah mutant (pink dose-response curve) relative to wild-type (blue).

would make the corresponding hydrogen bond with that tryptophan's backbone carbonyl. Here, structure-function studies using α-hydroxy acid substitution reveal that nicotine indeed makes a functional hydrogen bond with this backbone carbonyl in α6β2. The interaction is further supported and quantified by a double mutant cycle analysis utilizing *N*'-methylnicotinium. In contrast, TC299423 shows at best a weak interaction with this carbonyl.

Results and Discussion

α-hydroxy acid substitution at Thr150 in α6β2‡. All studies make use of the previously described α6β2‡ construct, which contains mutations far removed from the agonist binding site that increase plasma membrane levels, in part, by facilitating transport out of the endoplasmic reticulum and to the cell surface.[23] To probe for a hydrogen bond to a backbone carbonyl, the residue at the *i+1* position is mutated to the corresponding α-hydroxy acid (Figure 1B).[26] In both α6β2‡ and α4β2, the residue *i+1* to Trp149 is Thr150. In the mutation to threonine α-hydroxy acid (Tah), the amide backbone becomes an ester backbone without affecting the side chain (Figure 1C). It is well established that an ester carbonyl is a significantly weaker hydrogen bond acceptor than an amide carbonyl.[27] In previous studies of several nAChR subtypes, this mutation has produced shifts in EC_{50} ranging from 3-fold to 27-fold.[13]

The results for substituting α6 Thr150 with Tah are summarized in Table 1. Importantly, ACh – which cannot make a conventional hydrogen bond to the backbone carbonyl – shows no significant effect. This establishes that the function of the receptor has not been degraded in some generic fashion by the backbone mutation. In sharp contrast, nicotine displays a 24-fold

Table 1. Investigating Hydrogen Bonding at α6β2‡ TrpB Carbonyl

ACh	EC_{50} (μM)	n_H	I_{max} (μA)	Fold-shift	N
Thr	0.16 ± 0.01	1.3 ± 0.1	0.32 - 3.8		10
Tah	0.20 ± 0.01	0.9 ± 0.1	0.48 - 3.3	1.3	10
Nicotine	EC_{50} (μM)	n_H	I_{max} (μA)	Fold-shift	N
Thr	0.11 ± 0.01	1.4 ± 0.1	0.19 - 2.7		16
Tah	2.7 ± 0.1	1.2 ± 0.1	0.09 - 2.7	24	10
TC299423	EC_{50} (μM)	n_H	I_{max} (μA)	Fold-shift	N
Thr	0.08 ± 0.01	1.1 ± 0.1	0.21 - 3.6		11
Tah	0.30 ± 0.01	0.9 ± 0.1	0.12 - 4.1	3.8	13

increase in EC_{50} (loss of function, dose responses shown in Figure 1D), suggesting it makes a potent hydrogen bond with the backbone carbonyl of TrpB. Perhaps surprisingly, only a 4-fold loss of function was observed for TC299423.

Quantifying the α6β2‡-nicotine Hydrogen Bond. Our results show that perturbing the backbone carbonyl at TrpB strongly impacts nicotine activation of the α6β2‡ receptor. This is highly suggestive of a hydrogen bond, but other explanations are possible. Also, putting an energetic value on the proposed hydrogen bond is challenging. A classic technique in determining a functional coupling interaction between amino acids in a protein is the double-mutant cycle analysis.[28–30] In this type of experiment, the two amino acids of interest are each mutated in a way that would attenuate the proposed interaction, both independently (as single-

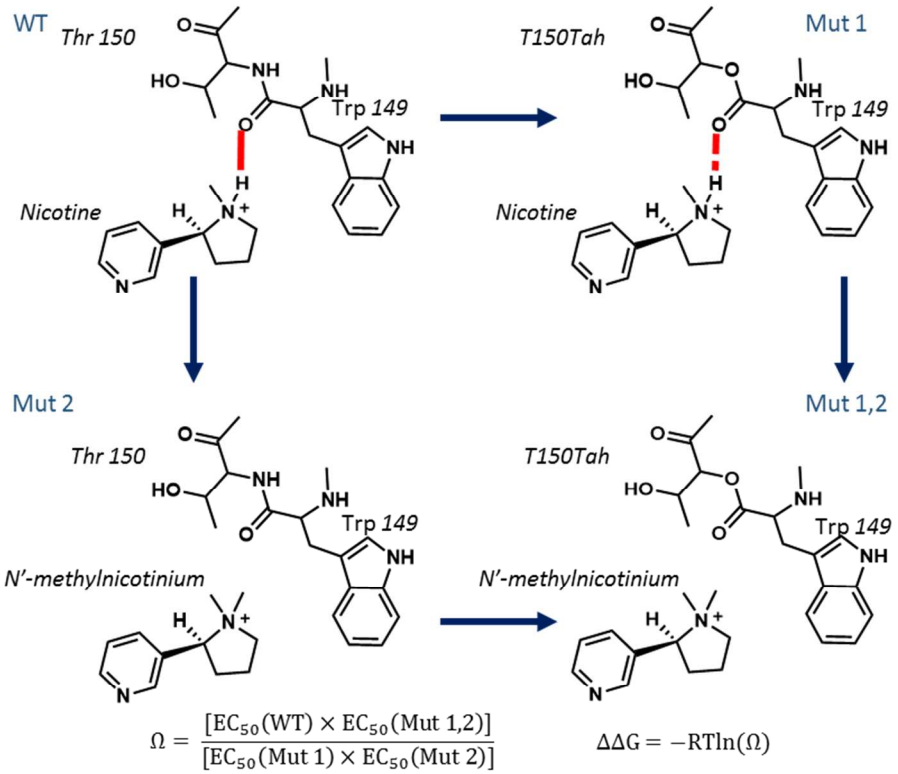

Figure 2. Schematic of the double-mutant cycle analysis used to confirm and quantify a functional hydrogen bond between nicotine at α6β2 receptors. Equations used to calculate Ω and ΔΔG values are shown.

mutants) and simultaneously (as a double-mutant). If the change in binding seen in the double-mutant is a simple sum of each single-mutant – that is, if the energetic effects are additive – the single-mutant perturbations act independently of each other, and the two amino acids do not participate in a functionally coupled interaction. If, on the other hand, the effect of the double-mutant proves to be non-additive, the amino acids are considered to be functionally coupled. The degree to which the double-mutant is additive or non-additive is expressed by an Ω value, which is defined as the product of the wild-type and double-mutant EC_{50} values divided by the product of the single-mutant EC_{50} values (Figure 2). An Ω value differing from 1 indicates functional coupling between amino acids. As discussed elsewhere, perturbations to EC_{50} resulting from mutations at the agonist binding site can be considered to reflect changes in agonist binding affinities, allowing an Ω value to be converted to a ΔΔG for the coupling energy between amino acids.[29,31–33]

To assess the nicotine hydrogen bond with the TrpB backbone carbonyl, we designed an analog to the double-mutant cycle analysis (schematic shown in Figure 2). The first mutant in the analysis is the T150Tah substitution that results in an amide-to-ester backbone mutation. The second "mutant" uses a nicotine analog, wherein the pyrrolidine nitrogen is methylated to yield *N*'-methylnicotinium (N'MeNic in data tables). As a quaternary ammonium, this compound is similar to ACh in that it is unable to donate a hydrogen bond. By finding EC_{50} values for each condition – nicotine at wild-type, nicotine at T150Tah, *N*'-methylnicotinium at wild-type, and *N*'-methylnicotinium at T150Tah – and determining whether or not the double-mutant shows an additive loss of function, this mutant cycle will not only further test the hypothesis that nicotine makes a hydrogen bond with the backbone carbonyl of Trp149 but will also quantify the strength of the hydrogen bond. We have previously used a similar mutant cycle analysis – one mutation

being on the protein the other on the drug – to probe the hydrogen bond involving the pyridine N of nicotine.[30]

As a proof of concept, the double-mutant cycle analysis described above was first performed in the α4β2 nAChR, because this subtype is more extensively studied and has a better understood binding map for nicotine. At α4β2, nicotine shows a 27-fold shift in EC_{50} at the T150Tah mutant, a major loss of function (Table 2). When N'-methylnicotinium is tested at the wild-type receptor, a 6-fold loss of function is observed. If these two mutations were independent of each other - meaning loss of function was due to an effect other than attenuating the proposed hydrogen bond - an additive loss of function would be expected at the double-mutant close to 160-fold. Instead, an EC_{50} of 0.40 μM is observed, which is not meaningfully different from the EC_{50} of N'-methylnicotinium at wild-type (0.62 μM) and only a 4-fold loss of function compared to nicotine at the wild-type. This lack of additivity is quantified with an Ω value of 42, which when expressed in free energy terms reveals a ΔΔG value of -2.2 kcal/mol. This value is comparable to empirically determined hydrogen bond strengths of *N*-methylacetamide aggregates in carbon tetrachloride (ΔH^o = -4.2 kcal/mol) and benzene (ΔH^o = -3.6 kcal/mol).[34,35]

The same approach was taken in α6β2‡; as noted above nicotine experiences a 24-fold loss of function at T150Tah. The other single-mutant in this analysis, which is N'-methylnicotinium at wild-type α6β2‡, shows an even larger loss of function, with a 38-fold shift in EC_{50}. If these losses in function were not due to hydrogen bonding and instead were independent of each other, the double-mutant fold-shift would be additive with a nearly 900-fold increase in EC_{50} with respect to wild-type. The double-mutant, N'-methylnicotinium at T150Tah, has instead an EC_{50} of 1.2 μM, an 11-fold shift away from wild-type, showing the effect is non-additive. Overall, the mutant cycle has an Ω value of 88 and a ΔΔG of -2.6 kcal/mol, suggesting nicotine makes a hydrogen bond in α6β2‡ that is at least as strong as that seen in α4β2.

Conclusion

These results reveal an interesting diversity among nAChR subtypes. First, consider the binding of nicotine at the two different receptor subtypes – α4β2 and α6β2. The binding pattern for α4β2 is familiar – a strong cation-π interaction to TrpB and a strong hydrogen bond to the

Table 2. Double Mutant Cycle Analysis of the Nicotine-TrpB Carbonyl Hydrogen Bond

α4β2	Agonist	T150	EC_{50} (μM)	n_H	I_{max} (μA)	Fold-shift	N
WT	Nic	Thr	0.10 ± 0.01	1.4 ± 0.2	0.05 - 1.2	1	15
Mut1	Nic	Tah	2.7 ± 0.1	1.3 ± 0.1	0.11 - 1.2	27	6
Mut2	N'MeNic	Thr	0.62 ± 0.03	1.2 ± 0.1	0.02 - 0.60	6.2	10
Mut1,2	N'MeNic	Tah	0.40 ± 0.04	1.1 ± 0.1	0.08 - 0.42	4.0	12
						Ω	**42**
						ΔΔG (kcal/mol)	**-2.2**

α6β2‡	Agonist	T150	EC_{50} (μM)	n_H	I_{max} (μA)	Fold-shift	N
WT	Nic	Thr	0.11 ± 0.01	1.4 ± 0.1	0.19 - 2.7	1	16
Mut1	Nic	Tah	2.7 ± 0.1	1.1 ± 0.1	0.09 - 2.7	24	10
Mut2	N'MeNic	Thr	4.2 ± 0.2	1.0 ± 0.1	0.10 - 2.1	38	11
Mut1,2	N'MeNic	Tah	1.1 ± 0.1	0.9 ± 0.1	0.08 - 1.1	11	10
						Ω	**88**
						ΔΔG (kcal/mol)	**-2.6**

associated backbone carbonyl. In α6β2 the cation-π interaction is absent, and so one might conclude that the drug had moved away from TrpB. We now find that nicotine makes a comparably strong hydrogen bond to the backbone carbonyl in α6β2 – a surprising and intriguing binding pattern. Another interesting difference is seen in the consequences of quaternizing nicotine – making it more like the natural agonist ACh. In α4β2 this has a modest effect on potency (only a 6-fold shift), but in α6β2 the impact is markedly larger (a 37-fold shift), again suggesting an altered binding orientation.

Finally, our results suggest that TC299423 interacts very weakly with TrpB. There is no evidence for a cation-π interaction, and backbone mutation has a much smaller effect than was seen for nicotine. These findings should provide valuable guidance to efforts to develop subtype-specific drugs targeting α6-containing nAChRs.

Corresponding Author: Dennis A. Dougherty, dadougherty@caltech.edu

Acknowledgements. This work was supported by the NIH (NS 34407, DA019375). MRP was supported by an NIH/NRSA training grant: 5 T32 GM07616. We thank Merouane Bencherif and Daniel Yohannes (Targacept) for gifts of TC299423.

Materials and Methods

Molecular Biology

Rat α6, α4, and β2 nAChRs were in the pGEMhe vector, a cDNA plasmid optimized for protein expression in *Xenopus* oocytes. Site-directed mutagenesis was performed by PCR using the Stratagene QuikChange protocol and primers ordered from Integrated DNA Technologies (Coralville, IA). Circular cDNA was linearized with SbfI (New England Biolabs, Ipswich, MA) and then transcribed *in vitro* using T7 mMessage mMachine kit (Life Technologies, Santa Clara, CA), with a purification step after each process (Qiagen, Valencia, CA). Final concentrations were quantified by UV spectroscopy.

Ion Channel Expression and α-hydroxy Acid Incorporation

For optimized expression, α4L9'Aβ2 and α6L9'Sβ2L9'$S_{LFM/AAQA}$ were used as the "wild-type" receptor which further mutations are compared against. These are referred to as α4β2 and α6β2[‡] respectively throughout for clarity. For nonsense suppression-based, site-specific non-canonical amino acid incorporation, the cyanomethylester form of threonine α-hydroxy was first synthesized, coupled to the dinucleotide dCA, and enzymatically ligated to UAG-suppressor 74-mer THG73 $tRNA_{CUA}$ as previously described.[13] The product was verified by MALDI time-of-flight mass spectrometry on a 3-hydroxypicolinic acid matrix. *Xenopus laevis* oocytes (stage V to VI) were sourced from both a Caltech facility and Ecocyte Bio Science (Austin, TX). The Tah-tRNA was injected along with T150UAG mRNA into oocytes at a 1:1 volume ratio, with an α6:β2 mRNA mass ratio of 10:1 or an α4:β2 mass ratio of 1:3, resulting in 25 ng each of mRNA and tRNA injected per cell. Cells were incubated 24-48 hours at 18°C in ND96 solution (96 mM NaCl, 2mM KCl, 1 mM $MgCl_2$, and 5mM HEPES, pH 7.5) enriched with theophylline, sodium pyruvate, gentamycin, and horse serum. The fidelity of incorporation of Tah was confirmed by charging tRNA with Thr in a wild-type recovery experiment. Data from these experiments (reported as Thr in the data tables above) matched wild-type data, reported in previous studies. A read-through/reaminoacylation test serves as a negative control wherein a 76-mer tRNA is injected alongside mRNA. Lack of current proved no detectable re-aminoacylation at the Thr150 site.

N'-methylnicotinium Synthesis

Synthesis of *N'*-methylnicotinium was based on previously reported methods.[36] All reagents were purchased from Sigma Aldrich (St. Louis, MO). In a roundbottom flask, 19.8 mL of (-)-nicotine were added to 250 mL of acetonitrile and excess sodium carbonate. Then, 5.76 mL of methyl iodide were added dropwise while stirring. The reaction was stirred at room temperature for three days. The reaction solution was filtered by vacuum and solids were discarded. Solvent from the filtrate was removed by rotary evaporation until tan oil remained. Deionized water, 50 mL, was added to the oil and dissolved forming an orange solution. Continuous chloroform extraction was performed on the orange solution for five days. The aqueous layer was isolated and solvent was removed by rotary evaporation upon which crystals formed. Product was recrystallized three consecutive times with hot isopropanol for an over 40% yield. Further purification was achieved by iterative preparative HPLC (Waters, Milford, MA) using a 100% water solvent profile.

^{1}H NMR (500 MHz, Acetonitrile-d_3) δ 8.80 (dd, J = 2.5, 0.8 Hz, 1H), 8.71 (dd, J = 4.8, 1.6 Hz, 1H), 8.12 – 8.00 (m, 1H), 7.50 (ddd, J = 8.0, 4.8, 0.9 Hz, 1H), 5.06 (dd, J = 11.5, 8.0 Hz, 1H), 3.95 – 3.69 (m, 2H), 3.12 (s, 3H), 2.75 (s, 3H), 2.74 – 2.63 (m, 1H), 2.57 – 2.42 (m, 1H), 2.39 – 2.19 (m, 2H).

Whole-Cell Electrophysiological Characterization

Acetylcholine chloride and (-)-nicotine tartrate were purchased from Sigma Aldrich (St Louis, MO), while TC299423 (Targacept) was a generous gift. *N'*-methylnicotinium iodide was prepared according to the procedure above. Agonist-induced currents were recorded in two-electrode voltage-clamp mode using the OpusXpress 6000A (Molecular Devices, Sunnyvale, CA) at a holding potential of -60 mV in a running buffer of Ca^{2+}-free ND96. Agonists were prepared

in Ca^{2+}-free ND96 and delivered to cells via a 1 mL application over 15 s followed by a 2 min wash. EC_{50} values describe the concentration required to activate half the receptors expressed on the cell surface and were determined through dose response experiments, while fold-shifts in EC_{50} are equal to the mutant EC_{50} divided by wild-type EC_{50}. To derive an EC_{50} value, data from dose-response experiments were normalized to the maximum current-response, averaged, and fit to the Hill equation using Kaleidagraph (Synergy Software, Reading PA), though data are visualized here with Prism (GraphPad Software, La Jolla, CA). Error bars, as well as reported errors for EC_{50} and Hill coefficient (n_H) are presented as SEM.

References

1. Quik, M. & Wonnacott, S. (2011) α6β2* and α4β2* Nicotinic Acetylcholine Receptors As Drug Targets for Parkinson's Disease. *Pharmacol. Rev.* **63,** 938–966.
2. Wonnacott, S. (1997) Presynaptic nicotinic ACh receptors. *Trends Neurosci.* **20,** 92–98.
3. Smart, T. G. & Paoletti, P. (2012) Synaptic Neurotransmitter-Gated Receptors. *Cold Spring Harb. Perspect. Biol.* **4,** a009662.
4. Le Novère, N., Corringer, P.-J. & Changeux, J.-P. (2002) The diversity of subunit composition in nAChRs: Evolutionary origins, physiologic and pharmacologic consequences. *J. Neurobiol.* **53,** 447–456.
5. Millar, N. S. (2003) Assembly and subunit diversity of nicotinic acetylcholine receptors. *Biochem. Soc. Trans.* **31,** 869–874.
6. Gotti, C., Zoli, M. & Clementi, F. (2006) Brain nicotinic acetylcholine receptors: native subtypes and their relevance. *Trends Pharmacol. Sci.* **27,** 482–491.
7. Zoli, M., Pistillo, F. & Gotti, C. (2015) Diversity of native nicotinic receptor subtypes in mammalian brain. *Neuropharmacology* **96,** 302–311.
8. Quik, M. & McIntosh, J. M. Striatal (2006) α6* Nicotinic Acetylcholine Receptors: Potential Targets for Parkinson's Disease Therapy. *J. Pharmacol. Exp. Ther.* **316,** 481–489.
9. Yang, K., Jin, G. & Wu, J. (2009) Mysterious α6-containing nAChRs: function, pharmacology, and pathophysiology. *Acta Pharmacol. Sin.* **30,** 740–751.
10. Holladay, M. W., Dart, M. J. & Lynch, J. K. (1997) Neuronal Nicotinic Acetylcholine Receptors as Targets for Drug Discovery. *J. Med. Chem.* **40,** 4169–4194.
11. Wieskopf, J. S. *et al.* (2015) The nicotinic α6 subunit gene determines variability in chronic pain sensitivity via cross-inhibition of P2X2/3 receptors. *Sci. Transl. Med.* **7,** 287ra72–287ra72.
12. Lester, H. A., Dibas, M. I., Dahan, D. S., Leite, J. F. & Dougherty, D. A. (2004) Cys-loop receptors: new twists and turns. *Trends Neurosci.* **27,** 329–336.
13. Van Arnam, E. B. & Dougherty, D. A. (2014) Functional Probes of Drug–Receptor Interactions Implicated by Structural Studies: Cys-Loop Receptors Provide a Fertile Testing Ground. *J. Med. Chem.* **57,** 6289–6300.
14. Dougherty, D. A. (2000) Unnatural amino acids as probes of protein structure and function. *Curr. Opin. Chem. Biol.* **4,** 645–652.
15. Xiu, X., Puskar, N. L., Shanata, J. A. P., Lester, H. A. & Dougherty, D. A. (2009) Nicotine binding to brain receptors requires a strong cation–π interaction. *Nature* **458,** 534–537.
16. Tavares, X. D. S. *et al.* (2012) Variations in Binding Among Several Agonists at Two Stoichiometries of the Neuronal, α4β2 Nicotinic Receptor. *J. Am. Chem. Soc.* **134,** 11474–11480.
17. Dougherty, D. A. (2013) The Cation−π Interaction. *Acc. Chem. Res.* **46,** 885–893.
18. Hassaine, G. *et al.* (2014) X-ray structure of the mouse serotonin 5-HT3 receptor. *Nature* **512,** 276–281.

19. Miller, P. S. & Aricescu, A. R. (2014) Crystal structure of a human GABAA receptor. *Nature* **512,** 270–275.
20. Huang, X., Chen, H., Michelsen, K., Schneider, S. & Shaffer, P. L. (2015) Crystal structure of human glycine receptor-α3 bound to antagonist strychnine. *Nature* **526,** 277–280.
21. Morales-Perez, C. L., Noviello, C. M. & Hibbs, R. E. (2016) X-ray structure of the human α4β2 nicotinic receptor. *Nature* **538,** 411–415.
22. Wall, T. R. (2015) Effects of TI-299423 on Neuronal Nicotinic Acetylcholine Receptors. Ph. D. Thesis, California Institute of Technology.
23. Post, M. R., Limapichat, W., Lester, H. A. & Dougherty, D. A. (2015) Heterologous expression and nonsense suppression provide insights into agonist behavior at α6β2 nicotinic acetylcholine receptors. *Neuropharmacology* **97,** 376–382.
24. Puskar, N. L., Xiu, X., Lester, H. A. & Dougherty, D. A. (2011) Two Neuronal Nicotinic Acetylcholine Receptors, α4β4 and α7, Show Differential Agonist Binding Modes. *J. Biol. Chem.* **286,** 14618–14627.
25. Cashin, A. L., Petersson, E. J., Lester, H. A. & Dougherty, D. A. (2005) Using Physical Chemistry To Differentiate Nicotinic from Cholinergic Agonists at the Nicotinic Acetylcholine Receptor. *J. Am. Chem. Soc.* **127,** 350–356.
26. England, P. M., Zhang, Y., Dougherty, D. A. & Lester, H. A. (1999) Backbone Mutations in Transmembrane Domains of a Ligand-Gated Ion Channel: Implications for the Mechanism of Gating. *Cell* **96,** 89–98.
27. Deechongkit, S. *et al.* (2004) Context-dependent contributions of backbone hydrogen bonding to β-sheet folding energetics. *Nature* **430,** 101–105.
28. Horovitz, A. (1996) Double-mutant cycles: a powerful tool for analyzing protein structure and function. *Fold. Des.* **1,** R121–R126.
29. Daeffler, K. N.-M., Lester, H. A. & Dougherty, D. A. (2012) Functionally Important Aromatic–Aromatic and Sulfur−π Interactions in the D2 Dopamine Receptor. *J. Am. Chem. Soc.* **134,** 14890–14896.
30. Blum, A. P., Lester, H. A. & Dougherty, D. A. (2010) Nicotinic pharmacophore: The pyridine N of nicotine and carbonyl of acetylcholine hydrogen bond across a subunit interface to a backbone NH. *Proc. Natl. Acad. Sci.* **107,** 13206–13211.
31. Colquhoun, D. (1998) Binding, gating, affinity and efficacy: the interpretation of structure-activity relationships for agonists and of the effects of mutating receptors. *Br. J. Pharmacol.* **125,** 924–947.
32. Marotta, C. B., Lester, H. A. & Dougherty, D. A. (2015) An Unaltered Orthosteric Site and a Network of Long-Range Allosteric Interactions for PNU-120596 in α7 Nicotinic Acetylcholine Receptors. *Chem. Biol.* **22,** 1063–1073.
33. Miles, T. F., Bower, K. S., Lester, H. A. & Dougherty, D. A. (2012) A Coupled Array of Noncovalent Interactions Impacts the Function of the 5-HT3A Serotonin Receptor in an Agonist-Specific Way. *ACS Chem. Neurosci.* **3,** 753–760.

34. Klotz, I. M. & Franzen, J. S. (1962) Hydrogen Bonds between Model Peptide Groups in Solution. *J. Am. Chem. Soc.* **84,** 3461–3466.
35. Davies, M., Evans, J. C. & Jones, R. L. (1955) Molecular interaction and infra-red absorption spectra. Part 4 — Methyl acetamide. *Trans. Faraday Soc.* **51,** 761.
36. Seeman, J. I. & Whidby, J. F. (1976) The iodomethylation of nicotine. An unusual example of competitive nitrogen alkylation. *J. Org. Chem.* **41,** 3824–3826.

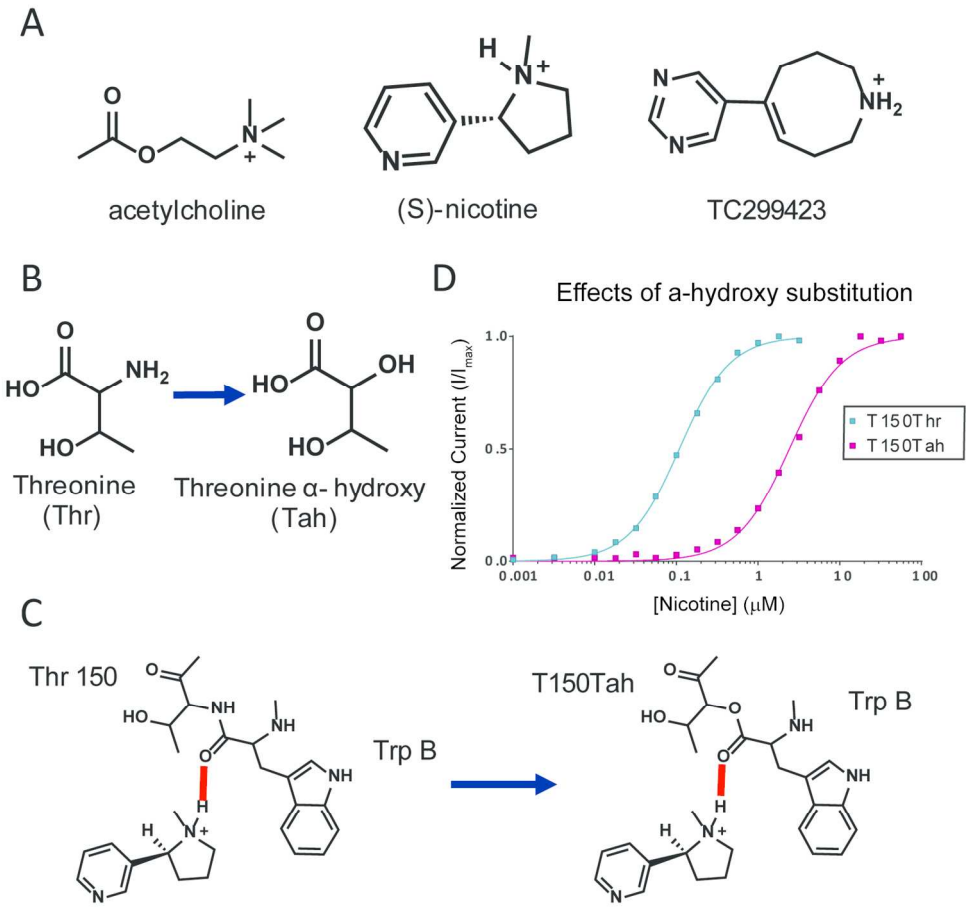

Figure 1

140x134mm (300 x 300 DPI)

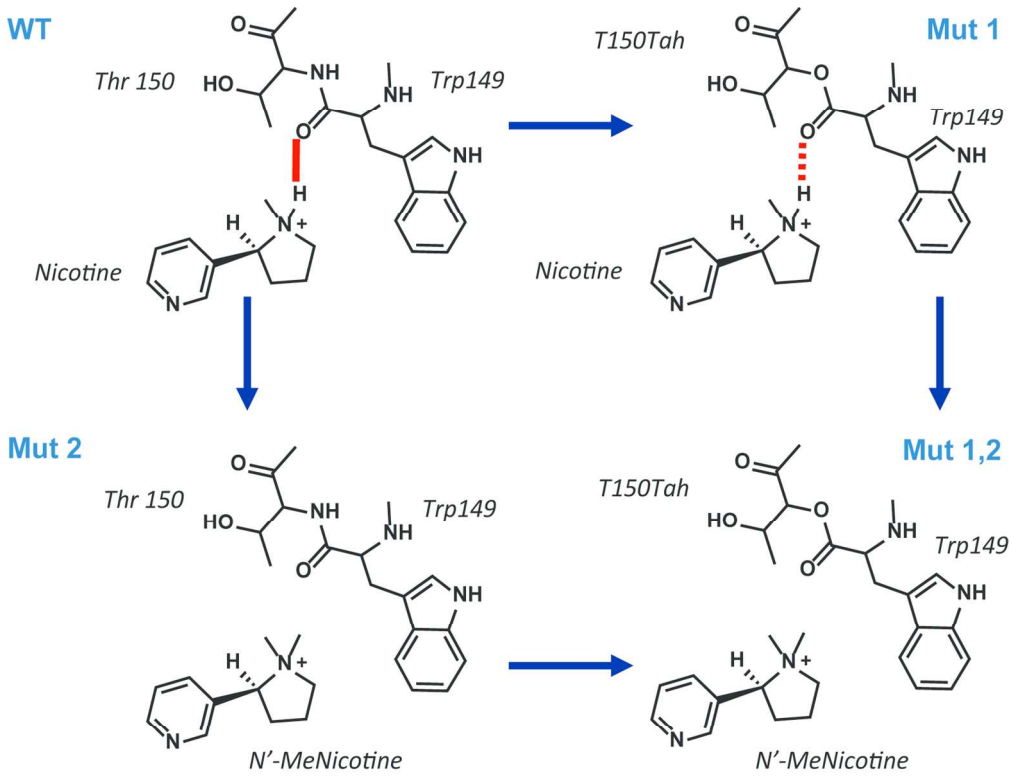

$$\Omega = \frac{[EC_{50}(WT) \times EC_{50}(Mut\ 1,2)]}{[EC_{50}(Mut\ 1) \times EC_{50}(Mut2)]} \qquad \Delta\Delta G = -RT\ln(\Omega)$$

Figure 2

134x124mm (300 x 300 DPI)

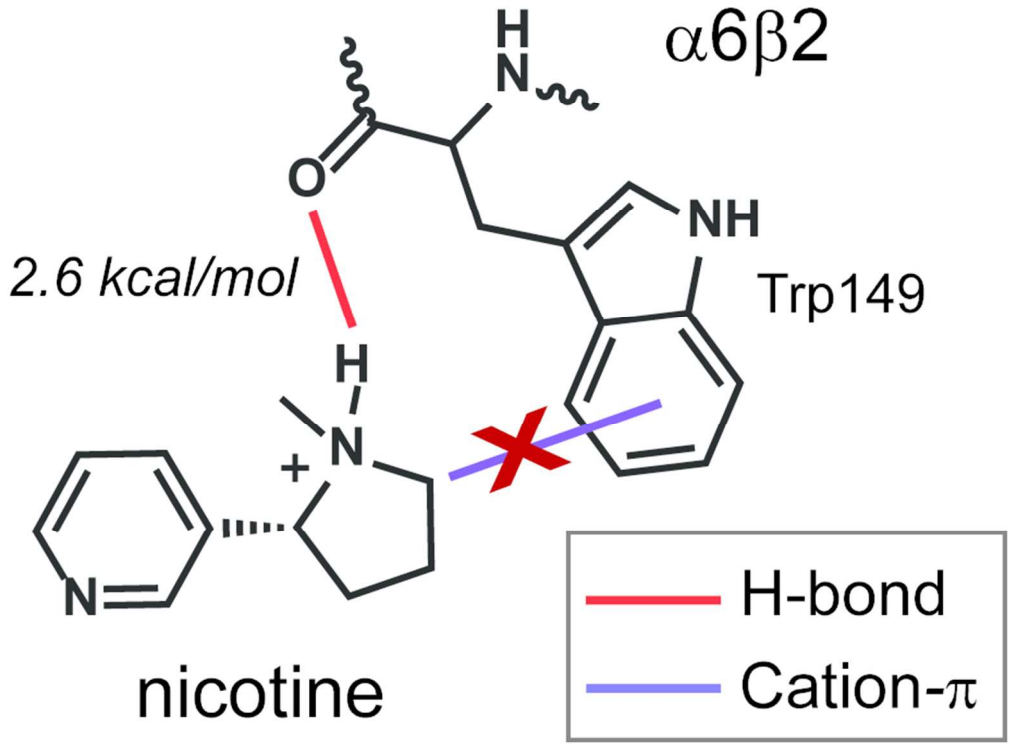

ToC graphic

77x58mm (300 x 300 DPI)